Molecular Crystals and Liquid Crystals Science and Technology. Section A. Molecular Crystals and Liquid Crystals

Publication details, including instructions for authors and subscription information:
http://www.tandfonline.com/loi/gmcl19

Manifestation of Charge Recombination Mechanisms in Electroluminescence of Organic Solids

J. Kalinowski [a]

[a] Department of Molecular Physics, Technical University of Gdańsk, ul. G. Narutowicza 11/12, 80-952, Gdańsk, Poland

Version of record first published: 24 Sep 2006

To cite this article: J. Kalinowski (2001): Manifestation of Charge Recombination Mechanisms in Electroluminescence of Organic Solids, Molecular Crystals and Liquid Crystals Science and Technology. Section A. Molecular Crystals and Liquid Crystals, 355:1, 231-245

To link to this article: http://dx.doi.org/10.1080/10587250108023663

Mol. Cryst. Liq. Cryst., Vol. 355, pp. 231-245
Reprints available directly from the publisher
Photocopying permitted by license only

Manifestation of Charge Recombination Mechanisms in Electroluminescence of Organic Solids

J. KALINOWSKI*

Department of Molecular Physics, Technical University of Gdańsk, ul. G. Narutowicza 11/12, 80–952 Gdańsk, Poland

(Received December 13, 1999; In final form February 07, 2000)

The electroluminescence (EL) emanated from organic light-emitting-diodes (LEDs) is demonstrated to provide quantitative information concerning recombination mechanisms in organic solids. Based upon the experimentally observed non-monotonic dependence of the quantum EL yield (φ_{EL}) on applied electric field (F) for molecularly-doped polymer hole transporting layer and Alq_3 emitter consisting LEDs, it is shown that while the low-field regime increase of $\varphi_{EL}(F)$ can be explained in the framework of the commonly used Langevin formalism, the high-field ($F>10^6$ V/cm) decrease in $\varphi_{EL}(F)$ requires to take into account a finite capture time of the carriers, which being comparable with the carrier motion time prior to the ultimate recombination step suggests the Thomson-like recombination to operate in organic solids. The electron-hole (CT) pair appears to be a plausible precursor of the ultimate recombination product (a localized neutral state). This is the branching ratio between its recombination decay (mutual carrier capture) and strongly field-dependent dissociation into free carriers that decides about φ_{EL} at high electric fields. It also accounts for the field value for which $\varphi(F)$ reaches its maximum.

Keywords: charge recombination; charge injection; electroluminescence; organic light-emitting-diodes; thin films

This paper is dedicated to Prof. Edgar Silinsh's Memory. He had continuously challenged the organic solid state community and his insights into electronic properties of molecular crystals will be kept in mind as having important impact on the organic solid state international community.

1. INTRODUCTION

Recombination of charge is one of the physical processes that need to be considered when setting up models aimed to understanding of photoconductive (PC), photoluminescence (PL) and electroluminescence (EL) properties of organic

* Corresponding Author.

molecular systems. The recombination process can be defined as a fusion of a positive (e.g. hole, h) and a negative (e.g. electron, e) charge carrier into an electrically neutral entity (e.g. exciton) which releases considerable amount of energy, and one of the problems that must be considered is how this energy is disposed of. If the oppositely charged carriers are generated independently far away each other, the volume-controlled recombination (VR) takes place, the carriers are statistically independent of each other, the recombination process is kinetically bimolecular. It usually leads to a charge pair state (CT) that decays to the ground state by the emission (k_f) of a photon ($h\nu$) plus some phonons (k_n), or exclusively by phonon emission. These processes are referred to as radiative and non-radiative recombination, respectively (Fig. 1). It is clear that various features of the recombination radiation bear information on the recombination process. Another way to infer about the VR process is to follow the concentration of mobile charge carriers by measurements of electrical conductivity. If, on the other hand, the CT pair is created as the first step in a molecular excited singlet (S^*) or triplet (T^*) state dissociation into free charge carriers process, the probability of the initial (geminate or unimolecular) recombination (IR) can be expressed by

$$P_R = 1 - \eta_0 \Omega, \tag{1}$$

where η_0 is the primary quantum yield in carrier pairs for the absorbed photon ($h\nu_{exc}$) and Ω is the (e-h) pair dissociation probability into independent carriers (Fig. 2). Since the probability of the initial recombination can be expressed by the charge separation step rates (η_0, Ω), the natural way of its determination is to measure the bulk-generated photocurrent. Another possibility to determine P_R is the electric-field-modulation of PL (EML). Elecric-field-effect on the effective charge separation efficiency ($\eta_0\Omega$) shows up in the varying population of CT states, and consequently, in the varying concentration of the molecular (Frenkel) excitons. It is expected that the field-induced increase in the charge separation efficiency would translate into quenching of light emitted either by CT and/or by localized excited states:

$$\delta = \varphi_{PL}(F)/\varphi_{PL}(0) = 1 - \eta_0 \Omega \tag{2}$$

Here $\varphi_{PL}(F)$ is the PL yield in the electric field F, and $\varphi_{PL}(0)$ is the PL yield at F=0, assuming k_f and k_n to be the field independent rate constants for radiative and non-radiative decay of excited states.

The recombination probability can be expressed in a more general way by the recombination time (τ_{rec}) and the carrier pair lifetime ($\tau_{e\text{-}h}$), the latter being determined by radiative or non-radiative rate constants of the pair, including that for dissociation into statistically independent carriers,

$$P_R = \left(1 + \frac{\tau_{rec}}{\tau_{e-h}}\right)^{-1} \tag{3}$$

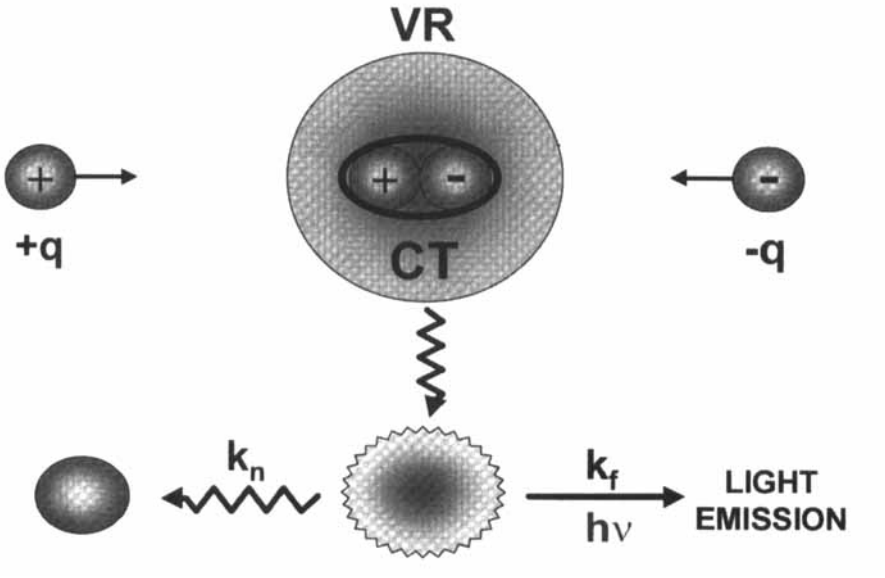

FIGURE 1 Volume-controlled recombination (VR) of statistically independent carriers (+q, -q)

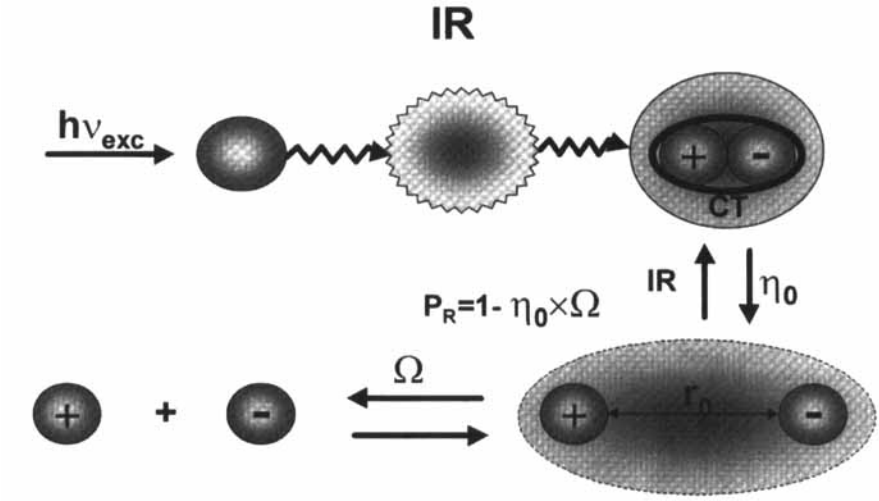

FIGURE 2 Initial recombination (IR) of a geminate (e...h) pair formed by absorption of light

The recombination time represents the sum of the motion time (τ_m), i.e. the time to get the carriers within capture radius (it is often assumed to be the coulombic radius $r_C=e^2/4\pi\varepsilon_0\varepsilon kT$), and the elementary capture time (τ_c) for the ulti-

mate recombination event (actual annihilation of charge carriers), $\tau_{rec}=\tau_m+\tau_c$. Following description of recombination processes in ionized gases a Langevin-like and Thomson-like recombination mechanisms can be introduced if $\tau_c \ll \tau_m$ and $\tau_c \gg \tau_m$, respectively. This paper is concerned with the problem whether charge carrier recombination in organic solids obeys the Langevin-like recombination formalism, as commonly assumed [1], or the Thomson-like recombination model applies under certain circumstances. Although photoconduction [2,3] and EML [4,5] studies have been carried out to infer about charge carrier separation processes by examination of the field dependence of the charge separation efficiency, $\eta_0\Omega$, there is no clear evidence for either of these mechanisms because $\eta_0\Omega$ determines the total recombination time,

$$\tau_{rec} = \tau_{e-h}\left[(\eta_0\Omega)^{-1} - 1\right]^{-1} \tag{4}$$

That is the tacit assumption $\tau_{rec}=\tau_m$ and $\tau_{e\text{-}h}(F)$=const which have led to the conclusion on the Lngevin-like recombination in organic solids.

In the present paper we show how the ratio $\tau_{rec}/\tau_{e\text{-}h}$ can be obtained without determination of the separation efficiency ($\eta_0\Omega$) of charge carrier pairs, examining charge carrier recombination as manifested directly in electroluminescence generated by electrons and holes injected from electrodes applied to thin organic films. The results are briefly discussed in terms of the Langevin- and Thomson-type recombination processes.

2. RECOMBINATION EL

Among various EL mechanisms electron-hole (e-h) recombination radiation seems to be most commonly discussed type of organic EL [6,7]. The holes injected from one of the electrodes of an organic emitter containing sandwich system, recombine within the emitter with electrons injected from the opposite electrical contact, and molecular emitting states are produced as shown in Fig. 1. Typical single layer (SL) EL structures comprise one transparent electrode (usually a glass substrate covered with an Indium-Tin-Oxide (ITO) thin layer anode), the organic luminescent film (Light Emitting Layer (EML)), and a metal (Al, Mg or Ca) cathode protected against atmospheric corrosion by a thick ($\cong$ 200nm) layer of Ag (see Fig. 3; more details concerning fabrication of organic EL devices can be found in various chapters of the Book cited in Ref. [6]). The quantum EL yield (φ_{EL}) appears to be one order of magnitude higher (up to 4% photon/electron) for a double-layer (DL) light-emitting-diodes (LEDs), where light emitting material is separated from one of the electrodes by a non-emitting charge transporting layer. In Fig. 3 these are 8-hydroxyquinoline aluminum complex (Alq_3) as EML and N,N′-diphenyl-N,N′-(3-methyl-1,1′-biphe-

nyl-4,4′-diamine (TPD) as a hole transporting layer (HTL). Dependent on quality of the electrical contacts the current (j)-voltage (U) characteristics of such LEDs show up as volume-controlled-currents (VCCs) given by the Parmentel-Ruppel's equation [8],

$$j_{VCC} = \frac{9}{8}\varepsilon_0\varepsilon\mu_{eff}\frac{U^2}{d^3} \tag{5}$$

where ε_0 is the dielectric permittivity of vacuum, ε is the dielectric constant, d is the sample thickness, and the effective mobility μ_{eff} is related to the so called recombination mobility $\mu_0=\varepsilon_0\varepsilon\gamma/2e$ (γ-second order recombination rate constant, e-elementary charge) in a complex manner [9], or as injection-controlled-currents (ILCs) which can take on different forms following different injection mechanisms [6]:

$$j_1(F) = AF^{3/4}\exp(aF^{1/2}), \tag{6}$$

a Schottky-type function for the field-assisted thermionic injection over the image force barrier,

$$j_2(F) = BF^2\exp(-b/F) \tag{7}$$

a Fowler-Nordheim-type function for carrier tunneling through a triangular barrier, and

$$j_3(F) = j_0\exp(-c/F^{1/2}) \tag{8}$$

for the hot carrier injection over the image force barrier.

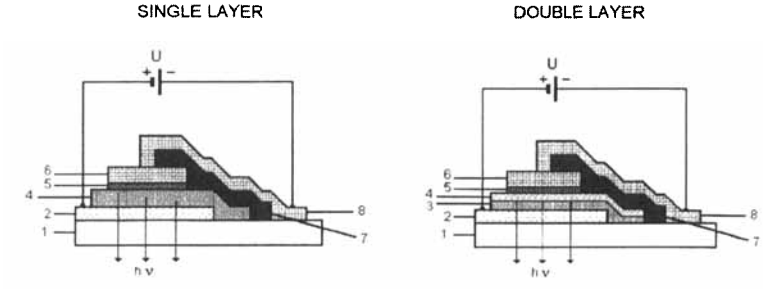

1 Glass substrate
2 Transparent anode (ITO ≈ 150 nm)
3 Hole transporting layer (HTL)
4 Light emitting layer (EML)
5 Cathode (Mg ≈ 20 nm)
6 Protective layer of Ag ≈ 200 nm
7 Insulating layer
8 Ag contact strip ≈ 200 nm

SINGLE LAYER (SL) TRUCTURES: ITO/Alq_3/Mg/Ag
ITO/TPD/Mg/Ag

DOUBLE LAYER (DL) TRUCTURES: ITO/TPD/Alq_3/Mg/Ag
↓ ↓
HTL EML

FIGURE 3 Schematic representation of typical sandwich type EL diodes

We note that equation (5) is not, generally, equivalent to unipolar space-charge-limited current (SCLC). It merges with SCLC only if $\mu_{eff}=\mu_e$ (or μ_h), that is when $\mu_e \gg \mu_0$ and $\mu_h \ll \mu_0$ (or $\mu_e \ll \mu_0$ and $\mu_h \gg \mu_0$), the less mobile carriers recombining very near the electrode from which they are injected. If the carrier mobility, μ, is in addition affected by an exponential distribution of carrier traps $h(E)=(H/kTI)\exp(-E/kT)$ with their total concentration H, and $I=(T_c/T)>1$ being the dimensionless parameter characterizing the decrease of h(E) with trapping energy E, the SCLC becomes a more steep function of voltage [1,9,10],

$$j_{SCLC} = N_{eff}\mu e(\varepsilon_0\varepsilon/He)^l U^{l+1}/d^{2l+1}, \tag{9}$$

where N_{eff} is the effective density of states.

Such a voltage dependence of the current has been fitted to the experimental data for the DL LEDs based on the TPD/Alq_3 junction [11,12], a high value of $I = 6 - 10$ being attributed to the presence of deep electron traps in the electron-transporting-layer (ETL) made of Alq_3. It is known that deep traps lead to location of EL emitting zones in anthracene and tetracene single crystals close to their electrical contacts [6,7]. In the case of $\mu_e,\mu_h \ll \mu_0$ (strong recombination limit), $\mu_{eff} \cong \mu_e+\mu_h$, we deal with the double-injection current characterized by negligible space-charge overlap. This case is improbable whenever the thermal release time from traps is greater than the recombination time ($\tau_{rel}>\tau_{rec}$). Finally, the injected plasma case can be distinguished for $\mu_e,\mu_h \gg \mu_0$(weak recombination limit). In this case the effective mobility is much larger than both electron (μ_e) and hole (μ_h) mobilities, and is given by [9]

$$\mu_{eff} = (2/3)[2\pi(\mu_e\mu_h/\mu_0)(\mu_e + \mu_h)]^{1/2} \tag{10}$$

The light emitting zone may then be extended throughout the whole emitter thickness.

From a kinetic model, assuming the excited states to be produced throughout the sample with arbitrary concentrations of electrons n_e and holes n_h, the photon flux per unit area emitted from the EL cell of thickness d can be expressed as

$$\Phi_{EL} = \varphi P_S \gamma n_e n_h d \tag{11}$$

where $\varphi=k_f/k_S$ is the emission quantum yield and $P_S$is the probability that in the recombination event a singlet excited state will be created. In trap-free (or shallow-trap) samples $P_S=1/4$ because due to spin statistics, three times more triplet than singlet excited states are created in the electron-hole recombination process [6,13]. The current behaviour of the EL light output defined by equation (11) is strongly dependent on carrier injection conditions. The cells working in the injection-controlled EL (ICEL) mode obey the relation [6,7]

$$\Phi_{EL} = \varphi\gamma P_S \frac{j_i^h j_i^e}{e^2 \mu_e \mu_h F^2} d \tag{12}$$

The EL output is here proportional to both hole (j_i^h) and electron (j_i^e) injection currents, resulting, generally, in a non-linear relationship between Φ_{EL} and cell driving current [6,7]. In contrast, the EL cells operating under volume-controlled EL mode (VCEL) reveal the linearity between EL output and driving current [6,7]

$$\Phi_{EL} = \frac{\varphi P_S}{\varepsilon_0 \varepsilon \gamma} \frac{\mu_e \mu_h}{\mu_{eff}} j \tag{13}$$

The driving current can be here identified with VCC (5) as generated by ohmic injection at both electrodes. However, the current linearity of Φ_{EL}cannot be considered as an unequivocal criterion to distinguish between ICEL and VCEL modes, since the ICEL mode operating cells reveal linear Φ_{EL}(j) plots under special injection conditions in the presence of an appropriate exponential distribution of traps [6]. It is important to point out that the non-linear Φ_{EL}(j) relationship indicates a current (thus field) dependent quantum EL yield related closely to the recombination mechanism operating in an organic solid (se Secs. 3 and 4).

3. EL EFFICIENCY. DETERMINATION OF $\tau_{REC}/\tau_{E\text{-}H}$

The quantum EL yield (φ_{EL}) comes from experimental data as the ratio of the photon flux per unit area (Φ_{EL}) to the carrier stream per unit area (j/e):

$$\varphi_{EL} = e\Phi_{EL}/j \tag{14}$$

It represents the number of photons of energy hν emitted per charge carrier passed through the EL cell. As far as the recombination EL is concerned, the EL yield is directly proportional to the recombination probability (3) and may be expressed as

$$\varphi_{EL} = \varphi_{PL} P_S P_R = \frac{\varphi_{PL} P_S}{1 + \tau_{rec}/\tau_{e-h}} \tag{15}$$

Once having the measured quantum EL yield, the $\tau_{rec}/\tau_{e\text{-}h}$ ratio can be obtained from Eq. (15) if the PL quantum yield (φ_{PL}) of the emitter and P_S are known. With non-linear relationship $\Phi_{EL} - j$ for the ICEL mode operating EL cells (see Sec. 2), $\varphi_{EL}$is expected to be a quantity dependent on electric field (F). In fact, φ_{EL} varying with field has been observed, the φ_{EL}(F) curves show maxima above 10^6 V/cm for both SL and DL LEDs [13,14]. An interesting example is shown in Fig. 4. Apart from evaporated 100% TPD HTL, the maxi-

mum shifts towards higher fields as concentration of TPD in the PC polymer binder (bisphenol-A-polycarbonate) decreases. At the same time the maximum value of $\varphi_{EL}(max)$ decreases by more than one order of magnitude. Since in the LEDs of Fig. 4 emission comes out from Alq_3 layer, the PL efficiency of Alq_3 films, $\varphi_{PL} \cong 12\%$ and $P_S = 1/4$ can be used to determine the ratio $\tau_{rec}/\tau_{e\text{-}h}$ from Eq. (15).

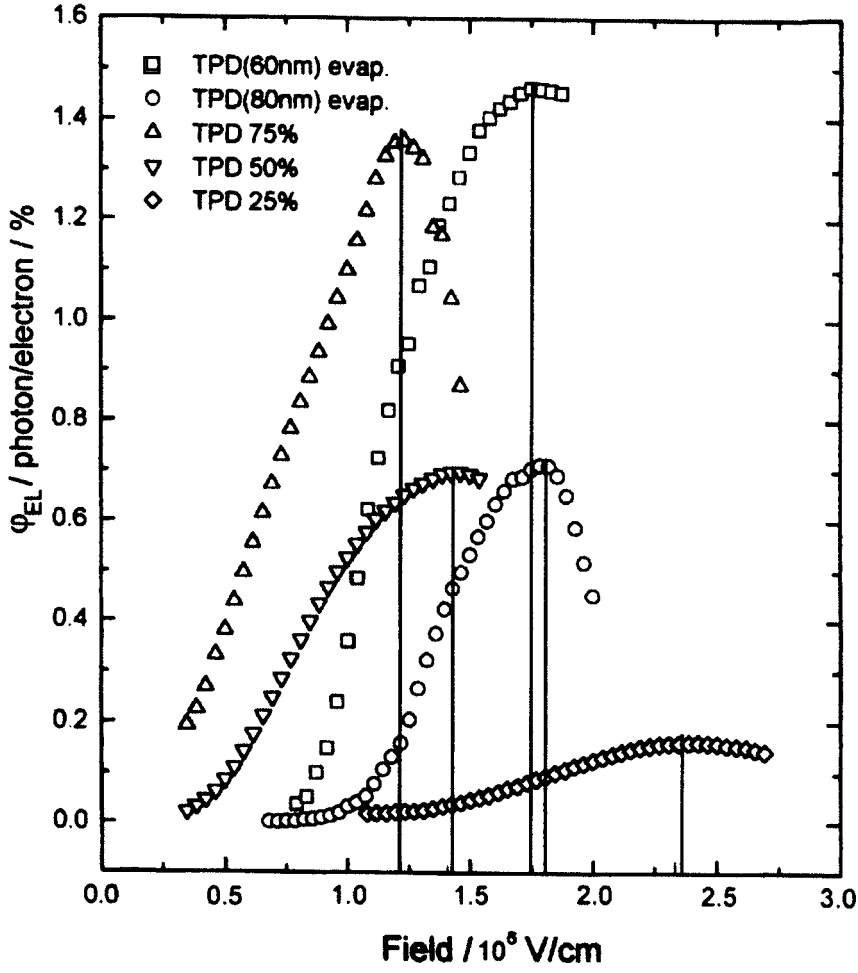

FIGURE 4 Quantum EL yield against applied field for a series of DL LEDs based on (PC+%TPD)/Alq_3 junction in a sandwich configuration (M. Cocchi, G. Giro, J. Kalinowski, P. Di Marco and V. Fattori as quoted in Ref. [13])

Apparent minima of the ratio correspond to observed maxima of $\varphi_{EL}(F)$ in Fig. 4 (see Fig. 5). The e-h (CT) pair lifetime ($\tau_{e\text{-}h}$) interpreted as the dissociation

time (τ_d) of the pair into independent electron and hole (see Fig. 2) is not sufficient to describe the overall recombination probability in the recombination process (Fig. 1). The probability of (CT) formation must be taken into account since decay of free carriers at electrodes competes naturally with the formation of CT pairs (Fig. 6). Hence, the total probability for recombination (P_R) should be a product of the probability of the formation ($P_R^{(1)}$) of the CT pair and the probability ($P_R^{(2)}$) of its conversion (ultimate recombination step – capture) into S_1or S_0 state,

$$P_R = P_R^{(1)} P_R^{(2)} = [1 + (\tau_m/\tau_t)]^{-1}[1 + (\tau_c/\tau_d)]^{-1} \tag{16}$$

In the common approach $\tau_c \to 0$ and $\tau_d \to \infty$ is assumed. Then, in the framework of the Langevin-type recombination with $\tau_{rec}=\tau_m=(\gamma\ n)^{-1}$, and $\tau_{e\text{-}h}=\tau_t=d/\mu F$ being the carrier transit time between electrodes,

$$\frac{\tau_{rec}}{\tau_t} = \frac{\tau_m}{\tau_t} = \frac{\mu_{e,h} F}{\gamma n_{h,e} d} \tag{17}$$

The observed decrease of the quantum EL yield by decreasing the concentration of TPD in PC, suggests the hole injection current to be responsible for the light output determined by the recombination of holes with electrons confined at the interface within a thin Alq_3 zone [15]. Thus, approximating j with $j_h=e\mu_h n_h F$, the ratio (17) can be expressed as

$$\frac{\tau_{rec}}{\tau_t} = \frac{8e\mu_e}{9\gamma\varepsilon_0\varepsilon} \frac{j_{SCL}}{j} \tag{18}$$

or using (5), as

$$\frac{\tau_{rec}}{\tau_t} = \frac{e\mu_h\mu_e F^2}{\gamma j(F) d} \tag{19}$$

Since in our example the diodes operate in the ICEL mode, that is $j<j_{SCL}$ and $dj(F)/dF>dj_{SCL}(F)/dF$ as comes from eqns. (5) and (6) to (8), τ_{rec}/τ_t decreases and φ_{EL} increases with electric field. This would agree with experiment (Figs. 4 and 5) for the lower field region ($F<10^6$V/cm) if $\mu_e(F)$=const and $(\mu_h/\gamma)(F)$=const were assumed. While the second condition is fulfilled by identifying τ_{rec} with τ_m, the μ_e appears to be an increasing Poole-Frenkel-type function of electric field $\mu_e(Alq_3)=\mu_{e0}\exp(\beta_e F^{1/2})$ with $\beta_e \cong 7.4\times10^{-3}(cm/V)^{1/2}$ [16]. On the other hand, the field increasing injection current in the (PC+%TPD)/Alq_3 junction-based LEDs, which have been shown to follow well the one-dimensional Onsager model of injection (see Eq. (6)) with $a>10^{-2}$ $(cm/V)^{1/2}$ [7], make the τ_{rec}/τ_t still monotonically decreasing, and, consequently, φ_{EL} a monotonically increasing function of electric field. The apparent disagreement with this prediction follows from the high-field region (above maximum φ_{EL} and minimum

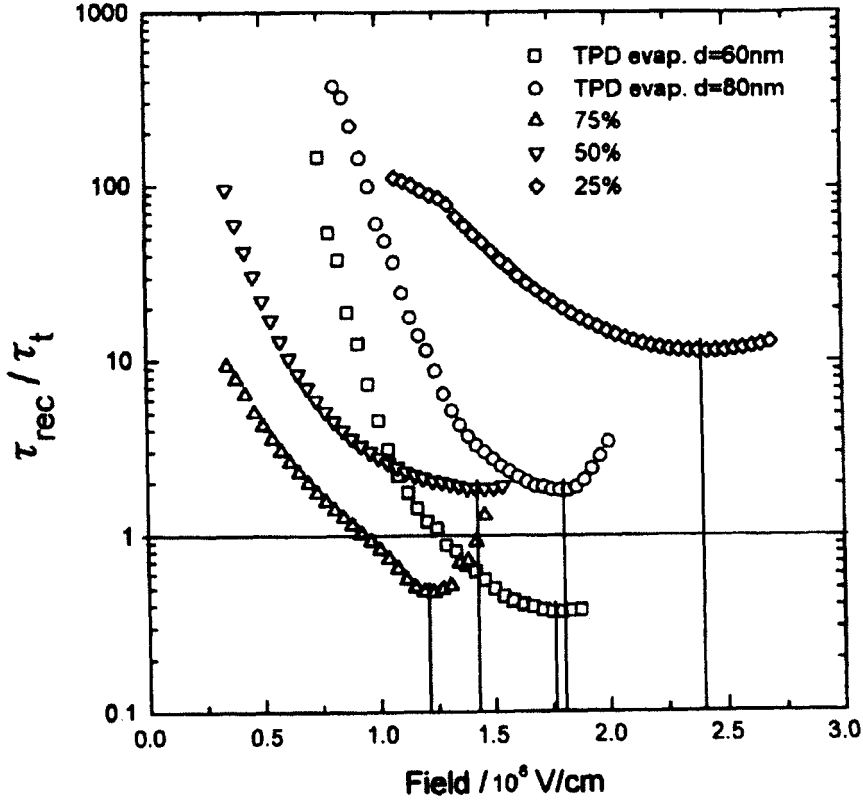

FIGURE 5 The τ_{rec}/τ_t ratio as a function of electric field for the LEDs from Fig. 4

τ_{rec}/τ_t), where φ_{EL} decreases and τ_{rec}/τ_t increases with electric field. We believe that the decrease of the φ_{EL} at large electric fields is due to a strongly enhanced dissociation of CT pairs. This translates into the field decreasing dissociation time, τ_d, which makes the ratio τ_c/τ_d meaningful with respect to unity; φ_{EL} is now dominated by decreasing $P_R^{(2)}$ imposed by the field increasing capture-to-dissociation time ratio (τ_c/τ_d) (see Eq. (16)).

4. LANGEVIN VERSUS THOMSON RECOMBINATION

The results of Sec. 3 allow to distinguish two limiting cases for the ICEL: (i) the EL with the mobility and charge carrier injection efficiency driven φ_{EL} ($\tau_c/\tau_d \ll 1$)

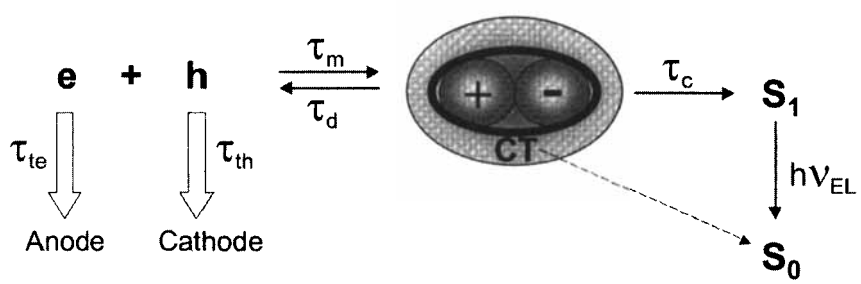

FIGURE 6 The three-step kinetic scheme of the VC recombination, taking into account free carriers decay at electrodes, formation of CT pairs and emitting excited singlet states S_1

and (ii) the EL governed by the lifetime of the e-h (CT) pairs formed in the recombination process of statistically independent charge carriers ($\tau_{rec}/\tau_t \ll 1$). The first case, by definition, corresponds to the Langevin-like (μ/γ=const), the second case to the Thomson-like recombination process as discussed in Sec. 1. In the framework of Eq. (16), the initial increase of φ_{EL} is due to a decrease of τ_{rec}/τ_t (19), τ_c/τ_din the low-field region being negligible. As the applied field is increased, the capture events will be stronger impeded and the τ_c/τ_d branching ratio increases inducing a decrease in $P_R^{(2)}$. At still higher fields the φ_{EL} increase observed at low field strengths is replaced by a decrease of the quantum EL yield upon increasing the field strength (Fig. 4). According to Eqs. (6), (15), (16) and (19)

$$\varphi_{EL}^{(lf)} \cong \frac{P_S \varphi_{PL}}{1 + C_1 F^{3/2} \exp[(\beta_e - a)F^{1/2}]} \tag{20}$$

in the low-field (If) approximation with $C_1=e\mu_h\mu_{e0}/\gamma Ad$, and

$$\varphi_{EL}^{(hf)} \cong \frac{P_S \varphi_{PL}}{1 + C_2 \exp(\beta_d F^{1/2})} \tag{21}$$

in the high-field (hf) approximation with $C_2=\tau_c/\tau_{d0}$.

In the latter case τ_d has been assumed to follow a Poole-Frenkel (PF) function, $\tau_d=\tau_{d0}\exp(\beta_d F^{1/2})$, where

$$\beta_d = \beta_{PF} = (e^3/\pi\varepsilon_0\varepsilon k^3 T^2)^{1/2} = 1.5 \times 10^{-2} (\mathrm{cm V^{-1}})^{1/2} \tag{22}$$

for Alq_3 with ε=3.8 at room temperature.

Fig. 7 compares the $\varphi_{EL}(F)$ plots for the ITO/(75%TPD:PC)/Alq_3/Mg device for low (a) and high (b) field regimes, in the $\log(\varphi_{EL}^{-1})$ versus $F^{1/2}$ representation (PF plots). It is obvious that PF behaviour is approached in the low- and high-field portions of the $\varphi_{EL}(F)$ dependence from Fig. 4. This means that φ_{EL}^{-1}

>> $(P_S\varphi_{PL})^{-1}$= (0.25 × 25%)$^{-1}$= =0.16/% as calculated with P_S=0.25 and φ_{PL}=25% [17]. The slope of the semilogarithmic plot φ_{EL}^{-1} against $F^{1/2}$ (Fig. 7a) yields β_e-a=-6.2×10^{-3}(cmV^{-1})$^{1/2}$, and using, as previously, β_e=0.74×10^{-2}(cmV^{-1})$^{1/2}$, leads to a ≅ 1.40×10^{-2}(cmV^{-1})$^{1/2}$. This value is in good agreement wit a ≅ 1.66×10^{-2}(cmV^{-1})$^{1/2}$ obtained independently from the current-field characteristics [7].

The value of $\beta_d \cong 1.3\times10^{-2}(\mathrm{cmV}^{-1})^{1/2}$ obtained from the high-field PF plot of $\log(\varphi_{EL}^{-1})$ (Fig. 7b) within the 15% accords with the PF coefficient β_{PF} (22). Extrapolating the linear portion of the $\log(\varphi_{EL}^{-1})^{(hf)}$ versus $F^{1/2}$ graph towards F=0 results in the capture-to-dissociation time ratio of CT states, $\tau_c/\tau_{d0}=C_2/P_S\varphi_{PL}$, of ≅10^{-3}. The dissociation time at zero applied field can be defined by a thermally activated process as

$$\tau_{d0} = \nu_0^{-1} \exp(\Delta E/kT), \tag{23}$$

where $\nu_0 \cong 10^{12}s^{-1}$ is a frequency factor, and

$$\Delta E = e^2/4\pi\varepsilon_0\varepsilon r_{CT} \tag{24}$$

is the activation energy. r_{CT} ranging from 3.5 Å (a closely located molecular pair) to 10Å, at room temperature, gives 0.43 eV ≥ ΔE ≥ 0.15eV (with ε=3.8). Thus, the values of τ_{d0} are between 0.3 ms and 0.4 ns, leading to a range of capture times, τ_c, between 0.3 μs and 0.1 ps, respectively. In light of this, the capture time (~ 0.3 μs) can be comparable with the carrier motion time τ_m, so that the Thomson-like recombination process is accessible in organic solids. Let us take the carriers to be injected into an Alq_3 layer of typical for LEDs thickness 100 nm. The carriers (here electrons) with mobility of the order of magnitude 10^{-4} cm^2/Vs (at F>10^6 Vcm^{-1}) [16] need $\tau_m \cong 0.1$ μs to pass the distance and to form CT pairs within the sample. The time lags between the field application time and the onset of EL in the TPD(60nm)/Alq_3(60nm) junction-based LEDs, observed experimentally, fall in this order of magnitude indeed [12]. Consequently, both the carrier motion time and its capture time contribute comparably to the overall recombination time. Since the quantum EL yield depends on the branching ratios τ_m/τ_t and τ_c/τ_d(cf. Eqs. (16), (20) and (21)), and these are decreasing and increasing functions of applied electric field, respectively, its maximum is expected for the field F_{max} when $\tau_m/\tau_t=\tau_c/\tau_d$,

$$F_{max} \cong [C/(a + \beta_d - \beta_e)]^2. \tag{23}$$

This can be rewritten as

$$\frac{1}{\sqrt{F_{max}}} \cong I + \frac{1}{C}a, \tag{24}$$

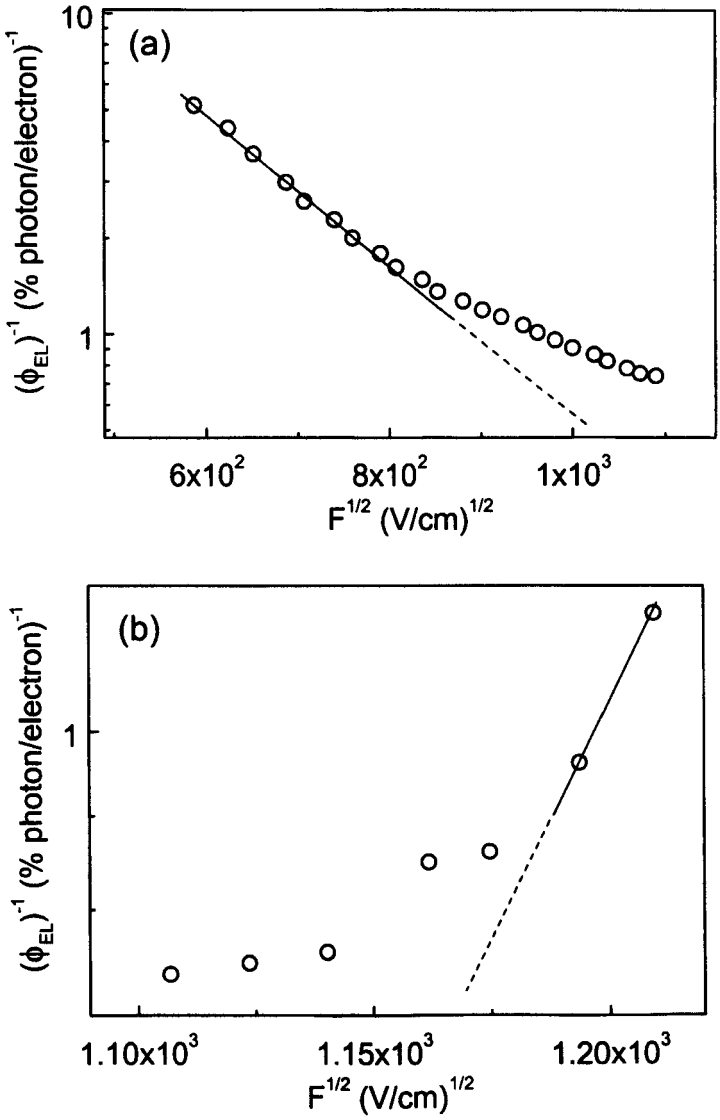

FIGURE 7 φ_{EL}(F) in $\log \varphi_{EL}^{-1}$ versus $F^{1/2}$ representation for the ITO/(75%TPD:PC/Alq_3/Mg/Ag LED in the low- (a) and high-field (b) regimes of the curve from Fig. 4

where $l = (\beta_d - \beta_e)/C$ and $C = \ln\left(e\mu_h\mu_{0e}F_{max}^{3/2}\tau_{d0}/\gamma A d\tau_c\right)$ is a slightly varying function of F_{max}. Recent electrical measurements on (%TPD:PC)/Alq_3 junctions

showed "a" to be an increasing function of concentration of TPD [7]. Their values for three (TPD:PC) HTL-based LEDs are represented in Fig. 8 by the abcissa values of the three figures standing for F_{max} taken from Fig. 4. As may be seen from Fig. 8, a linear plot of the reciprocal square root of F_{max} against injection parameter "a" is reasonably realized as predicted by Eq. (24) with $\beta_d - \beta_e = (1.3\times10^{-2} - 0.74\times10^{-2})(cmV^{-1})^{1/2} = 5.6\times10^{-3}(cmV^{-1})^{1/2}$. The agreement between the predictions of the analysis advanced above and experimental results allows to draw the reliable conclusions.

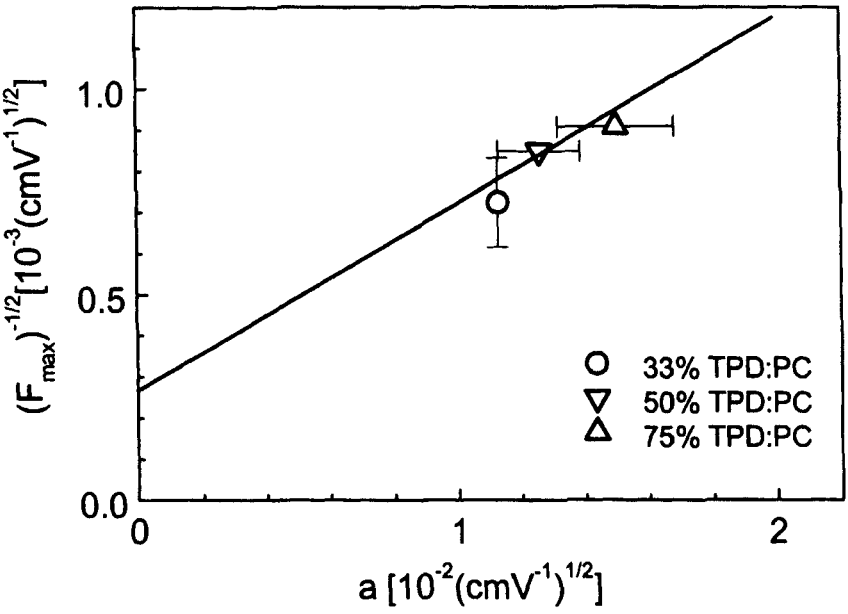

FIGURE 8 The field position (F_{max}) of the maxima of the $\varphi_{EL}(F)$ curves obtained for the DL LEDs based on (TPD:PC) HTL with different concentrations of TPD from Fig. 4. The straight line is the prediction of the model expressed by Eq. (24)

5. CONCLUSIONS

We have shown that EL characteristics of organic LEDs, being a direct manifestation of bimolecular charge recombination, allow to extract quantitative information concerning recombination mechanisms in organic solids. The exploration of field-dependent quantum EL yield of double-layer LEDs, completed with an analysis of their current-field characteristics provided arguments that both Langevin-like and Thomson-like recombination process is possible in molecular

condensed matter. A kinetic model for electron-hole recombination EL is presented. The quantum EL yield is shown to be governed by transport and carrier injection ability of electrodes at low fields and by the balance between capture and dissociation of electron-hole (CT) pairs formed in the recombination process at high fields ($F>10^6$ V/cm). The existence of these two limiting cases suggests that the recombination process within the low-field regime can be realistically approximated by the Langevin formulation assuming the carrier motion time prior to the ultimate recombination step (τ_m) to exceed substantially the capture time (τ_c), and that in the high-field regime to be approximated by the Thomson model assuming $\tau_c > \tau_m$. Comparison of the predicted EL yields with those measured experimentally makes it clear that the ultimate recombination step is the capture within relaxed CT states. The expected CT state radii are 1nm or less. The present results invalidate the common explanation of the recombination process in organic solids solely on the basis of carrier motion.

References

1. M. Pope and C.E. Swenberg, *Electronic Processes in Organic Crystals* (Clarendon, Oxford, 1982).
2. P.M. Borsenberger and A.I. Ateya, *J. Chem. Phys.* **49**, 4035 (1978).
3. T.E. Goliber and J.H. Perlstein, *J. Chem. Phys.* **80**, 4162 (1984).
4. J. Kalinowski, W. Stampor and P.G. Di Marco, *J. Chem. Phys.* **96**, 4136 (1992).
5. J. Kalinowski, W. Stampor and P. Di Marco, *J. Electrochem. Soc.* **143**, 315 (1996).
6. J. Kalinowski, in *Organic Electroluminescent Materials and Devices*, eds. S. Miyata and H.S. Nalwa (Gordon & Breach, Amsterdam, 1997) Ch. 1.
7. J. Kalinowski, *J. Phys. D: Appl. Phys.* **32**, R179 (1999).
8. R.H. Parmenter and W. Ruppel, *J. Appl. Phys.* **30**, 1548 (1959).
9. W. Helfrich, in *Physics and Chemistry of the Organic Solid State*, vol. III, eds. D. Fox, M.M. Labes and A. Weissberger (J. Wiley, New York, 1967) Ch. 1.
10. E.A. Silinsh, *Organic Molecular Crystals. Their Electronic States* (Springer, Berlin, 1980).
11. S.R. Forrest, P.E. Burrows and M.E. Thompson, in *Organic Electroluminescent Materials and Devices*, eds. S. Miyata and H.S. Nalwa (Gordon & Breach, Amsterdam, 1997) Ch. 13.
12. J. Kalinowski, N. Camaioni, P. Di Marco, V. Fattori and A. Martelli, *Appl. Phys. Lett.* **72**, 513 (1998).
13. J. Kalinowski, in *Multiphoton and Light Driven Multielectron Processes in Organics: New Phenomena, Materials and Applications*, eds. F. Kajzar and M.V. Agranovich (Kluwer, Dordrecht, 2000) p. 325.
14. G. Giro, M. Cocchi, J. Kalinowski, V. Fattori, P. Di Marco, P. Dembech and G. Seconi, *Adv. Mater. Optics and Electronics*, **9**, 189 (1999).
15. C.W. Tang, S.A. Van Slyke and C.H. Chen, *J. Appl. Phys.* **65**, 3610 (1989).
16. T. Tsutsui, H. Tokuhisa and M. Era, *Proc. SPIE* **vol. 3281**, 230 (1998).
17. H. Mattoussi, H. Murata, C.D. Merritt, Z.H. Kafafi, Y. Iizumi and J. Kido, *J. Appl. Phys.* **86**, 2642 (1999).